Hindawi
International Journal of Corrosion
Volume 2018, Article ID 6278542, 8 pages
https://doi.org/10.1155/2018/6278542

Research Article

Developing Field Test Procedures for Chloride Stress Corrosion Cracking in the Arabian Gulf

Hanan Farhat

College of the North Atlantic-Qatar, Doha 24449, Qatar

Correspondence should be addressed to Hanan Farhat; hanan.sharef@gmail.com

Received 21 January 2018; Revised 22 April 2018; Accepted 15 May 2018; Published 7 June 2018

Academic Editor: Francisco Javier Perez Trujillo

Oil and gas production and petrochemical plants in the Arabian Gulf are exposed to severe environmental conditions of high temperature and humidity. This makes these plants susceptible to chloride-induced stress corrosion cracking (CSCC). The laboratory testing fails to provide the exact field environmental conditions. A cost efficient field test setup for CSCC was designed and developed for the Arabian Gulf. The setup included designing self-sustained loading devices, samples, and sample racks. The samples were exposed to a stress equivalent to 80% and 100% of their yield strength. This paper describes the developed test procedures to establish testing with high level of accuracy and repeatability. It also discusses the design aspects and the challenges that were met.

1. Introduction

Chloride stress corrosion cracking (CSCC) takes place when specific alloys are exposed to tensile stress, temperature, and a chloride containing environment [1–3]. During CSCC, the alloy is attacked over most of its surface, while fine cracks progress through it [4]. Chloride stress corrosion cracking can occur fast when evaporation exists even at room temperature [5–9]. A number of catastrophic CSCC failures of roof construction in swimming pool environments has resulted in human causalities over the past decades [5, 6].

Several studies were performed in simulated field conditions for CSCC testing [10–21] as conventional laboratory tests did not represent the real field conditions. In one such a study, Turnbull et al. [13] managed to set new threshold temperature for CSCC of 22Cr and 25Cr duplex stainless steels under evaporation seawater conditions [13]. Yet, there is a continuous argument that laboratory test conditions can never represent the real field condition. The susceptibility to SCC depends on many environmental factors, including temperature variation during the day, concentration of chloride ions in the environment, which is a factor of the distance from the sea, and altitude above sea level [8, 9, 22]. The environment in the Arabian Gulf's oil and gas production sites is very corrosive and is characterized by high temperature and high humidity, representing continuous evaporation conditions in most of the year. Corrosion protection in these sites is very challenging. Most of the oil and gas installations are located near the sea, which in turn, enhances the build-up of chloride species on the surfaces of the alloys. Cases of severe CSCC in the region were reported [23]. These environmental conditions were difficult to replicate in the laboratory. This led to the need to develop a high accuracy field test setup for CSCC. One of the main objectives is to test the resistance of different corrosion resistance alloys to this cracking in the Arabian Gulf and to determine the actual time-to-CSCC failure of these alloys. Moreover, the impact of load and/or stress and temperature on the susceptibility to CSCC is to be investigated. To the author's knowledge CSCC field testing has never been applied in the Arabian Gulf before.

2. Materials and Methods

2.1. Material. Specimens from seven types of alloys were machined following NACE TM0177-2005 standard test method A [24]. The types of alloy, their yield strength, and elongation are given in Table 1.

The test was conducted at different stress levels to determine the threshold stress for CSCC. The load was applied using sustainable load devices (proof rings). The proof rings

Table 1: The alloys properties that were recorded from the tensile tests.

Specimen Type (UNS)	*Yield Strength (0.2% offset) (MPa)*	*Ultimate Tensile Strength (MPa)*	*Strain(mm/mm)*	*Reduction of Area (%)*
S30400	448	724	0.49	74
S31603	500	689	0.53	76
S32100	362	590	0.48	76
S32003	507	710	0.44	62
S32750	662	841	0.53	83
N08904	545	689	0.50	83
N08825	507	703	0.42	75

were manufactured from UNS 32205 duplex stainless steel, while the sample racks were made from aluminum 6061 alloy (UNS A96061). To apply the load on the samples, 316L stainless steel nuts were used. Detailed design and manufacturing procedures are provided in the results and discussion in Section 3.

The selection of test method A that includes the use of proof rings was made because the method is simple, compact, and easy. It provides flexibility in the choices of the size of the test specimen and range of stress levels. In addition, it can be used to determine the threshold stress for cracking, which is one of the objectives of this research study. NACE TM0177-2005 standard test method B for bent-beam test that follows ASTM G30 standards [25] is simple and economical. This method was ruled out because the actual stress distribution in the test specimen is not known. Therefore, the effect of different applied stresses cannot be studied using this method. Likewise, NACE TM0177-2005 standard test method C-Ring that follows ASTM G38 standards [26] was not used because of the difficulty of machining the test specimens in this method and the decreased precision in stressing, which is essential in this study [24].

3. Results and Discussion

3.1. Design Stress Calculations. Design stress calculation and analysis for the combination of specimen and proof ring under a load of 100% of the specimen's yield strength were performed using Solidworks software at room temperature. The analysis was conducted to determine the stress distribution on the samples and the proof rings. The samples and proof rings' material were identified in each stress analysis. The analysis was performed for two main tasks:

(i) The stresses have to be concentrated mainly on the samples' gauge length. Therefore the size of the sample has to be chosen carefully. The stress analysis was conducted on two sizes of specimens selected based on NACE TM0177-2005 standard [24]: (1) standard test specimen (gauge diameter is 6.35 ± 0.13 mm, and length is 25.4 mm) and (2) subsize test specimen (gauge diameter is 3.81 ± 0.05 mm, and length is 25.4 mm).

(ii) The proof rings should not be subject to high stresses that could cause their distortion and affect the amount of applied stress on the specimens.

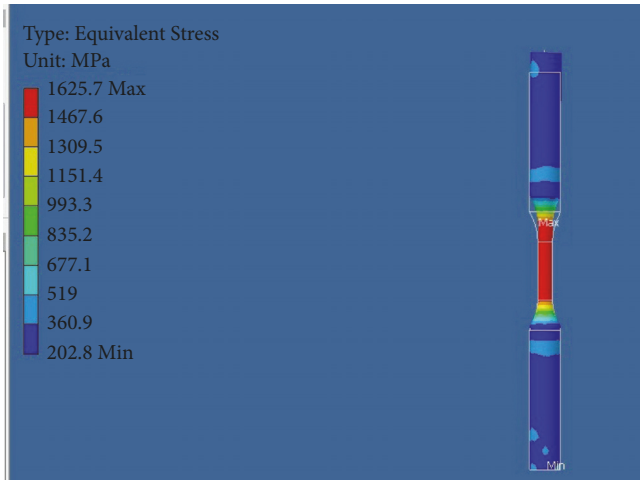

Figure 1: Design stress analysis for a subsize specimen showing the stress concentrating in the gauge length.

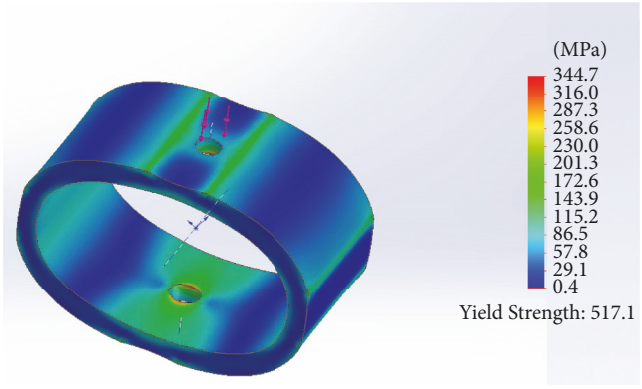

Figure 2: Design stress analysis for a proof ring 3" Schedule 80 pipe with the subsize specimen showing very small stresses around the hole.

Two sizes of proof rings were compared with a combination of two different specimens (subsize and standard specimen selected based on NACE TM0177-2005 standard [24]). The results of the stress analysis are presented in Figures 1–4. The stresses were found to concentrate in the specimen's gauge length as can be seen in Figure 1. The stresses increased whenever the colour changed from dark blue to red, as indicated by the load bar on the left of the figure. The increase

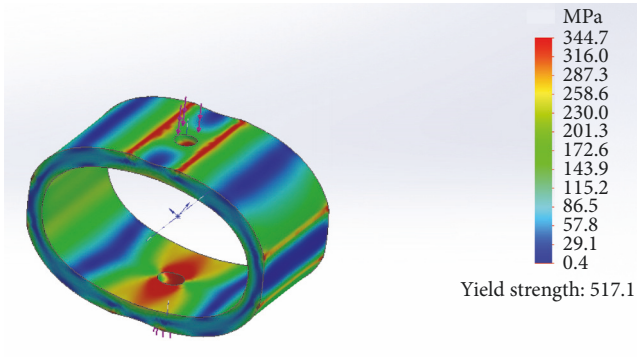

Figure 3: Design stress analysis for a proof ring 3" Schedule 80 pipe with the standard specimen showing more stresses covering a larger area around the holes.

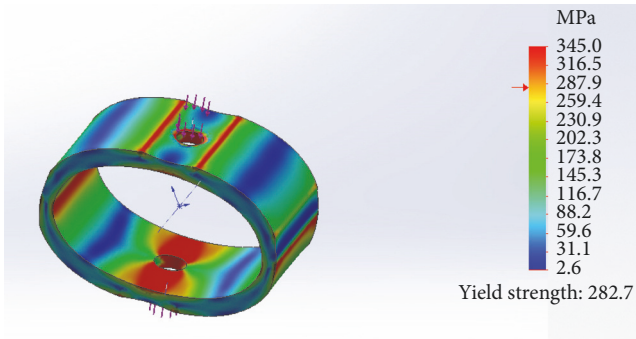

Figure 4: Design stress analysis for a proof ring 3" Schedule 40 pipe with the standard specimen showing large amount of stresses covering a larger area around the holes, and on the ring sides.

of stresses in the gauge length is to be expected, due to its smaller size compared to the rest of the specimen. This is the area where cracking and failure is expected to take place. The stress analysis on the proof rings, on the other hand, showed that when using the subsize samples, all the stresses in the ring were below yielding, except for the area around the hole, where localized higher stresses existed, as can be seen in red colour inside the hole in Figure 2. Still these stresses were in the acceptable limits and are below the proof ring's yield strength. In contrast, when using the standard specimen, the analysis showed higher stresses on wider areas around the holes as illustrated in Figure 3. These stresses are high stresses and are covering much wider region, compared to the stresses in the subsize specimen. Furthermore, the stress analysis on proof rings made from UNS 32205 duplex stainless steel – 3" Schedule 80 pipe (Figure 2) was compared with analysis of proof rings made from UNS 32205 duplex stainless steel – 3" Schedule 40 pipe (Figure 4). The subsize specimens were used in the two combination. The analysis results revealed that the rings that were made from 3" Schedule 80 pipe showed very minimum amount of stress, compared to very large stress that was noticed around the hole and on the sides of the rings in the specimens that were made from 3" Schedule 40 pipe. The stress analysis results made the base for the decision of choosing to use the subsize specimen instead of standard specimen and manufacturing the rings from 3" Schedule 80 pipe.

3.2. Design of Proof Rings. Sustained-load devices (proof rings) were used to apply load on the samples. The option of using coated or galvanized carbon steel pipe to make the rings was compared to the option of using duplex stainless steel pipe to make the rings. It was decided that applying coating on each induvial ring would be an expensive process and any defect or scratch in the coating could lead to galvanic corrosion of the carbon steel ring, and results in failing it, which may affect the load on the samples. Therefore, a UNS 32205 duplex stainless steel – 3" Schedule 80 pipe was used to make proof rings based on the stress analysis finding. The engineering drawing of the ring is illustrated in Figure 5.

3.3. Design of Test Specimens. The samples are designed following NACE TM0177-2005 standard [24]. The subsize tensile test specimen was chosen to be used based on the stress analysis results. One advantage this specimen has is that its small size enables shorter failure times compared to the standard size specimen, which will provide test results in a shorter time. Figure 6 illustrates the subsize specimen dimensions. Machining the samples was performed using Computer Numerical Control (CNC) machining following NACE TM0177-2005 standard [24], where the surface roughness was obtained by mechanical polishing and was ~ 0.21 μm. One hundred specimens from each alloy were machined to be placed in the field. After machining, the specimens were degreased with solvent and were cleaned in ethanol using ultrasonic cleaner. Gloves were used to handle the specimens to prevent the contamination of the gauge length. the specimens were stored in a desiccator until exposure.

3.4. Design of Sample Racks. The sample rack design took into consideration the test site location and environment. Wind speed was expected to reach a maximum of 32 m/s. The maximum deflection of each shelf was calculated to be 2.45 mm across the total length of 0.75 m. The racks were made from aluminum 6061 alloy (UNS A96061) to resist the corrosion in the sites. The shelves were tilted 30° with horizontal access to provide enough ambient exposure of all the specimens in the rack. Since different alloys will corrode/fail at different timing, each rack was designed so that it does not contribute to the applied load on the samples. Each rack accommodates 35 samples. Four racks were placed at each site to accommodate a total of 140 samples per site. In the onshore sites, each rack was fixed in a concrete stand to ensure that it will not get moved by the high wind. The racks that were placed offshore were bolted to the platforms. Figure 7 provides images of racks placed in onshore and offshore site.

3.5. Quality Control Testing. Several tests were conducted to control the quality of the samples, rings, and the sample racks. The tests included the following.

3.5.1. Visual Inspection. Using a 10X magnifier equipped with light, each sample was checked visually for any scratches or

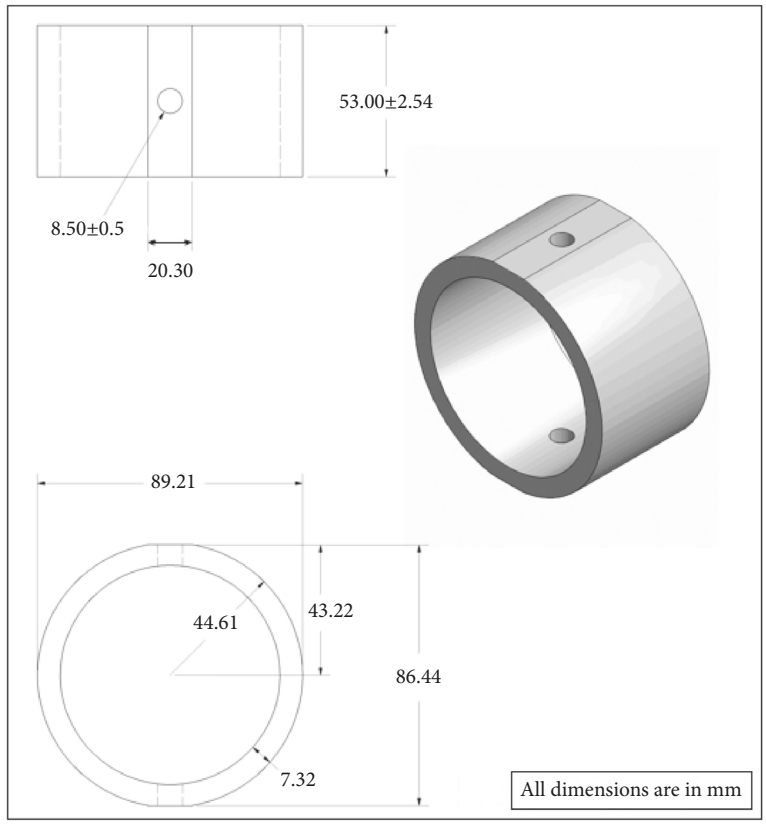

Figure 5: The design and dimensions of the proof rings.

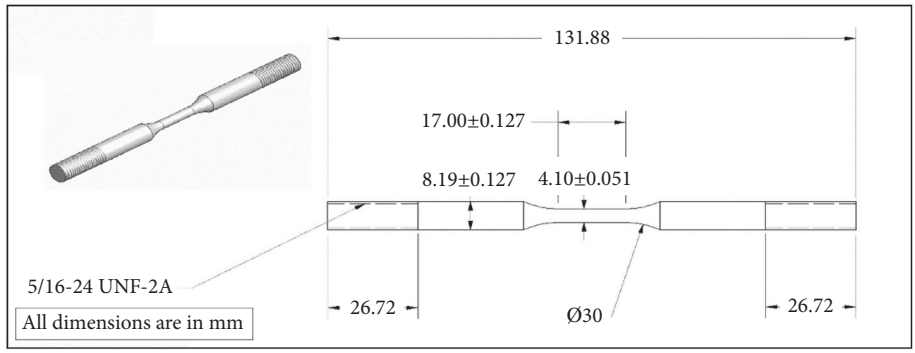

Figure 6: The dimensions of the subsize samples that were used in the CSCC field testing.

indentations in the gauge length. Few samples were noticed to have minor scratches in the gauge length area. These samples were excluded from field exposure, as scratches could act as preferred sites for pitting and cracking.

3.5.2. Tensile Testing of the Samples. Tensile testing was performed at room temperature. Three samples of each alloy were tested. A total of twenty-one stress-strain curves were generated. The results of this test are provided in Table 1. The yield strength of each alloy was identified as 0.2% offset. The average yield strength was calculated using the values that were measured in each sample. Values of 80% and 100% of the yield strength were recorded in each curve. The corresponding elongation was identified and used later, when applying loads to the samples.

3.6. Load Application. Seven hundred samples and rings were prepared to be placed in the field. Before applying the load, each sample and ring were given a code and the codes were engraved on the samples (away from the gauge length) and on the ring. The code indicates the type of alloy, applied load, exposure location, and the location in the sample rack (shelf number). Before applying the load the sample length was measured as follows.

3.6.1. Sample Length Measurement. The length of each sample was measured using two different methods. Overall length

(a) (b)

Figure 7: Sample racks (a) in onshore site and (b) in offshore site.

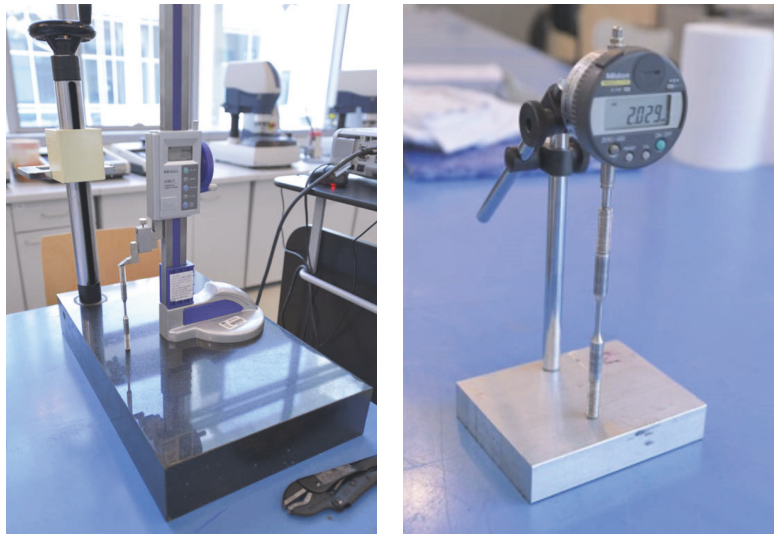

(a) (b)

Figure 8: (a) Digital height gauge used for length measurement noted to be operator dependent. (b) Lab built device for elongation measurement proved to be not dependent on operator with high degree of repeatability.

was measured using a rectangular surface plate and a digital height gauge (Figure 8(a)). The measurement was taken up to two millimeter decimal digits. This method resulted in some variation, operator dependence, and repeatability problems.

The second method was done using a lab built device that includes a digital indicator and two steel balls (Figure 8(b)). Each of the samples had been machined with a center drill taper in both ends. The process took advantage of the center drill taper. Measuring using the taper and the steel balls provided a means of measuring the change in specimen length relative to a base point. The device was calibrated before each measurement using a standard sample. Measurement technique was found to be not sensitive to the condition of the ends of each specimen and was not operator dependent and had a high degree of repeatability.

3.6.2. Load Application on the Samples. Once the samples were engraved and cleaned and their length was measured, they were assembled to their respective rings and hand tightened in place using two nuts on both sides. The nuts were AISI 316L stainless steel and were selected to fit a sample thread of 5/16" UNF.

Nuts from each type of alloy were difficult to find; therefore it was decided to use 316L stainless steel nuts. The use of 316L stainless steel nuts could cause galvanic corrosion between the specimens and nuts or the ring and nuts.

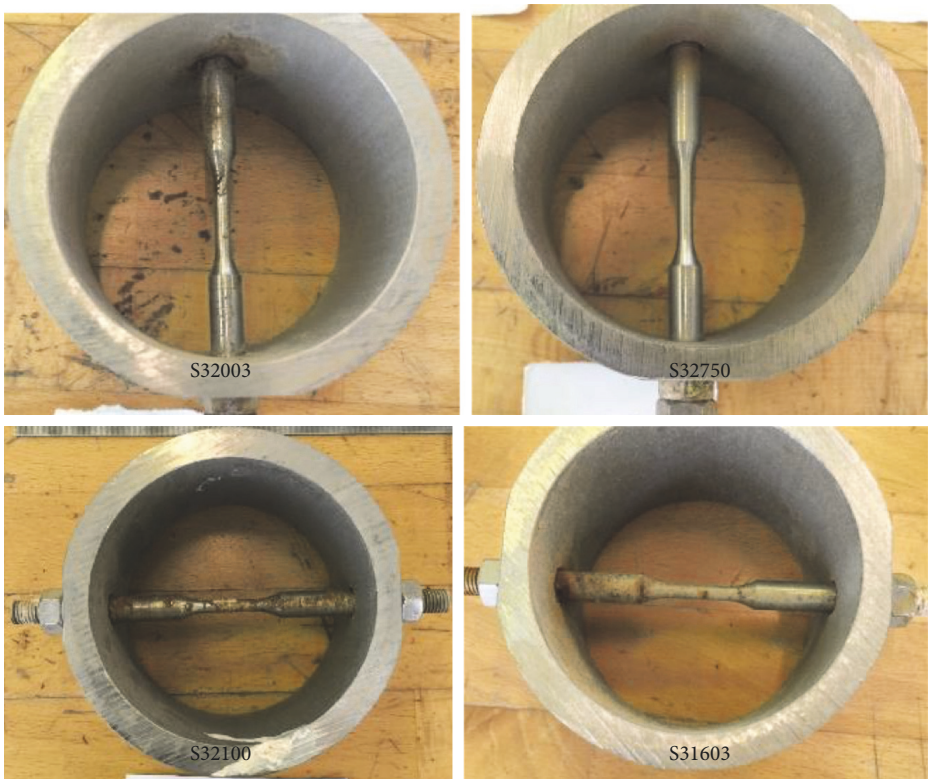

Figure 9: Retrieved samples after two years of exposure showing galvanic corrosion between some of the samples and the rings.

Attempts to use Teflon insulators did not work with the threaded nuts and samples. The nuts were greased before using and were observed during exposure for any signs of cracking or galvanic corrosion.

Each sample was torqued to a specific load using digital torque wrenches. The torque wrenches were calibrated before the application of the loads. Two loads were applied: 80% and 100% of the yield strength of the samples. The sample code indicates which load should be applied. Each load represented an elongation that was predetermined from the stress-strain curve of each alloy. The load application included the following steps:

(i) The 2 nuts at the bottom of the sample were tightened using a wrench.

(ii) A predetermined torque was applied to the top nut on the specimen. The torque produces an elongation that was determined from the stress-strain curve to reflect a specific load (80% or 100% yield strength).

(iii) The specimen was then placed back in the measuring fixture and the difference in the length was observed.

(iv) This procedure was repeated until the required change in specimen length was achieved.

(v) Once the required load and elongation has been attained, then the torqueing procedure is complete. All the measurement data is recorded and saved.

(vi) The sample is then kept aside for 7 days to allow enough time for cold creep, if any.

(vii) The sample's length was measured after 7 days and the difference in elongation between the last measured value and the present value was observed.

(viii) If the elongation was decreased, then the sample was torqued again using the same steps that were described above.

(ix) The final elongation was measured and recorded and the 4^{th} nut was tightened onto the sample using a wrench. This step completes the retorqueing procedure.

In order to overcome the possible torsion of the samples while applying the load, two aluminum sleeves were machined to fit around the samples (not the gauge length area). A vise grip was used to hold the sleeves in place. The sleeves were used so that the vise grip does not damage the sample surface. The vise grip is used to keep the sample from rotating and to prevent torsion.

The samples were placed in the sample racks and were exposed in the onshore and offshore environment. The samples were inspected once every month. The test was terminated when the samples failed. The failure was identified as either

(a) visual observation of cracks on the gauge length or

(b) complete separation of the test specimen.

During inspection, the nuts were also inspected for any signs of cracking. Galvanic corrosion was observed between some of the samples and rings as can be seen in Figure 9.

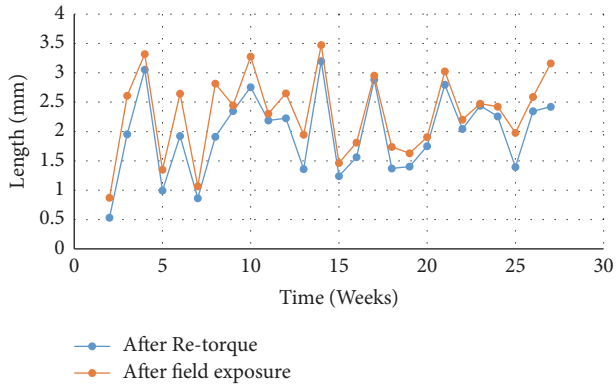

Figure 10: Comparison of samples' length measurements before and after exposure in one of the onshore sites showing no evidence of stress relaxation.

(a) (b)

Figure 11: Samples exposed in (a) offshore site and (b).

Alloy N08825 and alloy N08904 did not show any signs of galvanic corrosion. The galvanic corrosion was observed only outside the gauge length area and did not affect the CSCC testing. Galvanic corrosion was also observed between some of the samples and the nuts. The length of each sample was measured after retrieval. No reduction in length was observed, indicating that there was no stress relaxation and that the galvanic corrosion did not reduce the applied load on the samples. A slight increase in the length was observed. It could be attributed to expansion due to the heat that the samples were exposed to in the Middle East environment. The length measurement of samples that were exposed for two years in one of the onshore sites is provided in Figure 10. No cracking was observed in any of the nuts.

The test setup was used for over five years and proved to work efficiently in the Arabian Gulf environment, where the sample racks and proof rings survived the environmental conditions as can be seen in Figure 11. When comparing the cost of the test setup with the cost of buying individual proof ring devices, it is unmistakable that this test setup is cost effective.

4. Conclusions

A field exposure test setup was built for CSCC. The following conclusions were made:

(i) Sustained-load devices (Proof Rings) were efficient in applying loads of 80% and 100% yield strength on the samples.

(ii) The use of subsize specimens resulted in low stress levels on the proof rings, which in turn increased their durability and reduced their deformation during the testing.

(iii) Standard size specimens proved to produce a high stress level around the hole in the proof rings.

(iv) Rings made from UNS 32205 duplex stainless steel – 3" Schedule 80 pipe are subject to minor stresses compared to rings made from UNS 32205 duplex stainless steel – 3" Schedule 40 pipe, when the same load and specimen size are applied.

(v) The sample racks were found to withstand the environmental conditions in the Arabian Gulf. Their design allows for the removal and installation of samples without disturbing the loads on the tested specimens.

(vi) A lab built device that includes a digital indicator was successful in measuring the samples length and elongation and was not operator dependent and had a high degree of repeatability.

(vii) The field test set up proved to work well in the Arabian Gulf onshore and offshore sites and proved to be cost effective.

Data Availability

Data are available upon request.

Conflicts of Interest

The author declares that they have no conflicts of interest.

Acknowledgments

The author would like to thank Mr. Jim Fox, Ms. Vesna Covic-Palikuca, and Mr. Luay Hussein from the College of North Atlantic-Qatar for their contribution in the design and stress analysis. Thanks also are due to Dr. Roy Johnsen of the Norwegian University of Science and Technology, for his contribution to this research study, and to Qatar Petroleum, who made use of the field test set up and supported this study.

References

[1] D. A. Jones, *Principles and Prevention of Corrosion*, Prentice-Hall, NJ, USA, 1996, pp. 236-238.

[2] M. G. Fontana, *Corrosion Engineering*, McGraw-Hill, Singapore, 1987, pp. 109-112.

[3] S. A. Bradford, *Corrosion Control*, CASTI Publishing Inc., Bradford, England, 2004, pp. 171-174.

[4] Keneedy Space Center Corrosion Technology Laboratory, "Stress Corrosion Cracking," http://corrosion.ksc.nasa.gov/stresscor.htm, 2014.

[5] J. W. Oldfield and B. Todd, "Room temperature stress corrosion cracking of stainless steels in indoor swimming pool atmospheres," *British Corrosion Journal*, vol. 26, no. 3, pp. 173–182, 1991.

[6] J. W. Fielder, B. V. Lee, D. Dulieu, and J. Wilkinson, "The Corrosion of Stainless Steels in Swimming Pools," in *Applications of Stainless Steel '92*, vol. 2, pp. 762–772, Stockholm, Sweden, 9–11 June, 1992.

[7] R. B. Griffin, "ASM Handbook: Corrosion in Marine Atmospheres," 13C, pp. 42-57, 2005.

[8] M. E. R. Gustafsson and L. G. Franzén, "Dry deposition and concentration of marine aerosols in a coastal area, SW Sweden," *Atmospheric Environment*, vol. 30, no. 6, pp. 977–989, 1996.

[9] G. R. Meira, M. C. Andrade, I. J. Padaratz, M. C. Alonso, and J. C. Borba Jr., "Measurements and modelling of marine salt transportation and deposition in a tropical region in Brazil," *Atmospheric Environment*, vol. 40, no. 29, pp. 5596–5607, 2006.

[10] S. Huizinga, J. G. De Jong, W. E. Like, B. McLoughlin, and S. J. Paterson, "Offshore 22Cr Duplex Styainless Steel Cracking-Failure and Prevention," in *Corrosion 2005*, NACE International, Houston, TX, USA, 2005.

[11] U. Steinsmo, T. Rogne, and J. Drugli, "Aspects of testing and selecting stainless steels for seawater applications," *Corrosion*, vol. 53, pp. 955–964, 1997.

[12] H. Andersen, P. Arnvig, W. Wasielewska, L. Wegrelius, and C. Wolfe, "SCC of Stainless Steel under Evaporative Conditions," *Corrosion*, vol. 251, pp. 251/1–251/17, 1998.

[13] G. Hinds and A. Turnbull, "Threshold temperature for stress corrosion cracking of duplex stainless steel under evaporative seawater conditions," *Corrosion*, vol. 64, no. 2, pp. 101–106, 2008.

[14] A. Turnbull, S. Zhou, P. Nicholson, and G. Hinds, "Chemistry of concentrated salts formed by evaporation of seawater on duplex stainless steel," *Corrosion*, vol. 64, no. 4, pp. 325–333, 2008.

[15] A. Turnbull, P. Nicholson, and S. Zhou, "Chemistry of concentrated salts formed by evaporation of formation water and the impact on stress corrosion cracking of duplex stainless steel," *Corrosion*, vol. 63, no. 6, pp. 555–560, 2007.

[16] A. Almubarak, M. Belkharchouche, and A. Hussain, "Stress corrosion cracking of sensitized austenitic stainless steels in Kuwait petroleum refineries," *Anti-Corrosion Methods and Materials*, vol. 57, no. 2, pp. 58–64, 2010.

[17] L. Caseres and T. S. Mintz, "Atmospheric Stress Corrosion Cracking Susceptibility of Welded and Unwelded 304, 304L, and 316L Austenitic Stainless Steels Commonly Used for Dry Cask Storage Containers Exposed to Marine Environments," U.S.NRC Report, 2010.

[18] C. Ornek, X. Zhong, and D. L. Engelberg, "Low-Temperature environmentally assisted cracking of grade 2205 duplex stainless steel beneath a MgCl2:FeCl3 salt droplet," *Corrosion*, vol. 72, no. 3, pp. 384–399, 2016.

[19] L. Miller, T. S. Mintz, X. He et al., "Effect of Stress Level on the Stress Corrosion Cracking Initiation of Type 304L Stainless Steel Exposed to Simulated Sea Salt," https://www.nrc.gov/docs/ML1322/ML13220A332.pdf, 2013.

[20] B. M. Gordon, "Outside Diameter Stress Corrosion Cracking of stainless Steel in Light Water Reactors," in *Corrosion 2013*, NACE Int., Houston, TX, USA, 2013.

[21] T. S. Mintz, X. He, L. Miller et al., "Coastal Salt Effects on the Stress Corrosion Cracking of Type 304 Stainless Steel," in *Corrosion 2013*, NACE Int., Houston, Texas, 2013.

[22] Y. Toshima, Y. Ikeno, Y. Fujiwara, and Y. Nakao, "Long-Term Exposure Test for External Stress Corrosion Cracking on Austenitic Stainless Steels in Coastal Areas," in *Corrosion 2000*, NACE Int., Houston, TX, USA, 2000.

[23] P. A. Barker and H. H. Bech, "Material Selection for Threaded Instrument Fittings in Topside Offshore Service in the Arabian Gulf," in *Proceedings of the SPE International Production and Operations Conference & Exhibition*, Doha, Qatar, 2013.

[24] NACE, *Standard Test Method TM0177-2005: Laboratory Testing of Metals for Resistance to Sulfide Stress Cracking and Stress Corrosion Cracking in H_2S Environments*, NACE Int., Houston, TX, USA, 2005.

[25] ASTM, *G30-97: Standard Practice for Making and Using U-Bend Stress-Corrosion Test Specimens*, ASTM Int., West Conshohocken, 2009, pp. 1-7.

[26] ASTM, *G38-01: Standard Practice for Making and Using C-Ring Stress-Corrosion Test Specimens*, ASTM Int., West Conshohocken, 2013, pp. 1-8.